Cross-sectional imaging of spin injection into a semiconductor

P. KOTISSEK[1], M. BAILLEUL[1,2], M. SPERL[1], A. SPITZER[1], D. SCHUH[1], W. WEGSCHEIDER[1], C. H. BACK[1] AND G. BAYREUTHER[1]*

[1]Institut für Experimentelle und Angewandte Physik, Universität Regensburg, 93040 Regensburg, Germany
[2]Institut de Physique et Chimie des Matériaux de Strasbourg, UMR 7504 ULP-CNRS, 23 rue du Loess, BP 43, 67034 Strasbourg, France
*e-mail: guenther.bayreuther@physik.uni-r.de

Published online: 7 October 2007; doi:10.1038/nphys734

Recent discoveries of phenomena that relate electronic transport in solids to the spin angular momentum of the electrons are the fundamentals of spin electronics (spintronics). The first proposed conceptual spintronic device, the spin field-effect transistor—which has not yet been successfully implemented—requires the creation and detection of spin-polarized currents in a semiconductor. Whereas electrical spin injection from a ferromagnetic metal into GaAs has been achieved recently, the detection techniques used up to now have drawbacks like the requirement of large magnetic fields or limited information about the spin polarization in the semiconductor. Here we introduce a method that, by observation across a cleaved edge, enables us to directly visualize fully remanent electrical spin injection into bulk GaAs from a ferromagnetic contact, to image the spin-density distribution in the semiconductor in a cross-sectional view and to separate the effects of spin diffusion and electron drift.

Spintronics—the field of electron-transport phenomena related to the spin angular momentum of the electron—has experienced a rapid evolution in recent years, fed by the discovery of exciting new effects as well as by promise for novel electronic devices with new functionalities[1]. The spin field-effect transistor (spin-FET), first proposed in ref. 2, is still considered to be the paradigm of spintronic devices. As in a conventional FET, the conductivity of a semiconductor channel in a spin-FET is controlled by a voltage applied to the gate electrode. However, owing to the source and drain electrodes being ferromagnetic, the current in the channel is spin polarized and, hence, is also affected by the relative orientation of the magnetization in both electrodes and the electric field from the gate due to spin–orbit coupling effects[2]. Electrical spin injection into a semiconductor as the first requirement for the implementation of such a device has recently been achieved by inserting a Schottky barrier[3–6] or a tunnel barrier[7,8] between a ferromagnetic metal source contact and the semiconductor. To detect the spin polarization in the semiconductor most experiments up to now have used the spin-LED technique by measuring the degree of circular polarization of the luminescence light emitted after the recombination of spin-polarized electrons with (non-polarized) holes in a quantum well[1,3–5,7,8]. For narrow quantum wells, this technique requires that both the electron spins and the optical analysis direction be oriented along the surface normal to use the optical selection rules. The magnetization of the ferromagnetic source contact therefore must be tilted out of plane by a large magnetic field or by an intrinsic magnetic anisotropy with perpendicular easy axis[9,10]. Spin injection from an in-plane magnetized Fe film into GaAs has recently been demonstrated for a spin-LED by increasing the width of the quantum well from 10 to 100 nm and by measuring the circular polarization of recombination radiation in an edge-emission geometry[11].

Recently, it was shown that magneto-optic techniques can be used to detect the spin polarization of injected electrons from an in-plane magnetized ferromagnetic film[6]. A small in-plane magnetic field was applied perpendicular to the (in-plane) magnetization of the Fe contact and the polar magneto-optic Kerr effect used to measure the oscillatory transverse component of the spin polarization. The authors of ref. 6 have recently succeeded in extending their experiment to a purely electrical detection of spin polarization in a non-local geometry[12].

In the present work we introduce a novel method, which in addition to directly observing spin injection from an in-plane magnetized ferromagnetic film into bulk GaAs with 100% remanence enables us to measure the two-dimensional spin-density distribution in a cross-sectional view within the entire semiconductor and even below the ferromagnetic contacts. This is achieved by scanning across a cleaved edge of the sample with a magneto-optic Kerr microscope. The combination of features of this approach is expected to greatly facilitate the future development of semiconductor-based spintronic devices, and the implementation of a fully functional spin-FET in particular.

CROSS-SECTIONAL VIEW OF A SPINTRONIC DEVICE

The semiconductor into which spins are injected consists of a 4-μm-thick n-doped GaAs layer (doping density $n = 10^{16}\,\mathrm{cm}^{-3}$) grown by molecular beam epitaxy on top of a semi-insulating GaAs(001) substrate (see Fig. 1a for the sample design) followed by a thin n^+-GaAs film and the ferromagnetic metal contact layer. This guarantees the formation of a narrow Schottky barrier through which electron transport occurs by tunnelling[4]. A 14-nm-thick body-centred cubic (b.c.c.-) $Fe_{32}Co_{68}$(001) film epitaxially grown on the n^+-GaAs(001) layer was chosen for the source and drain contacts. Superconducting quantum interference device (SQUID)

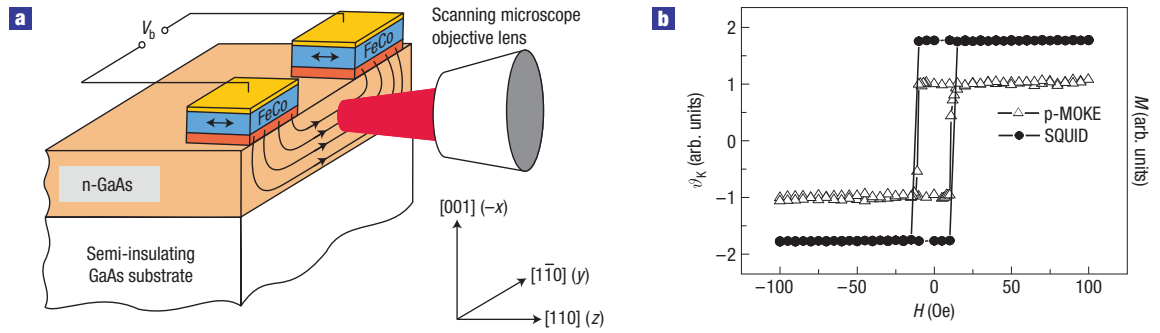

Figure 1 Schematic diagram of the spin-injection experiment (lateral transport) and basic magnetic behaviour. a, Schematic sample design and the detection method of the spin polarization in the semiconductor. The red layer below the Au-covered FeCo contact pads (blue) represents a 15-nm-thick n^+-GaAs layer ($n = 4 \times 10^{18}$ cm^{-3}) and a 15-nm-thick transition layer ($n \rightarrow n^+$). The focus of the Kerr microscope objective lens is scanned across the x–y plane, which is a (110) surface produced by cleaving the wafer across the metallic contacts. The final contact dimensions are 400 μm along the x axis and 100 μm along the z axis. The distance between the contacts is 600 μm. **b**, Magnetization loop, $M(H)$, of the FeCo(001) contacts at temperature $T = 10$ K measured by SQUID magnetometry with the magnetic field along [110] (solid circles) and Kerr rotation in the n-GaAs channel versus magnetic field ($H \parallel [110]$) for $T = 9$ K at a distance of 1 μm from the edge of the left FeCo ('source') contact for a bias voltage of $V_b = -1{,}300$ mV (open triangles). [110], that is the z axis, is the easy axis of magnetization for both the fourfold ('cubic') and the substrate-induced uniaxial magnetic anisotropy.

magnetometry of both $Fe_{32}Co_{68}$ contacts (200 μm × 400 μm patterned by optical lithography at a distance of 600 μm from each other) shows a rectangular hysteresis loop along the [110] direction with 100% remanence and a coercive field of about 15 Oe (Fig. 1b, solid circles). The current–voltage characteristics, $I(V)$, of individual junctions are in good agreement with a semiclassical model for tunnelling through a Schottky barrier[13] (see the Supplementary Information). Finally, the sample was cleaved along the [1$\bar{1}$0] direction across the FeCo pads, thus exposing the (110) surface, which enables direct optical access to the semiconductor channel. The magnetization of the ferromagnets is spontaneously aligned along [110], that is, perpendicular to the cleaved edge. This is the easy axis of magnetization both of the fourfold in-plane anisotropy and of the uniaxial interface anisotropy, as shown earlier[14]. For the optical measurements the sample was mounted on the cold finger of a He flow cryostat and the objective lens of a polarizing microscope was scanned across the cleaved edge, providing a spatial resolution of about 1.6 μm. The z component of the electron spin polarization (that is, the component along [110]) in the n-GaAs channel is detected via the polar magneto-optical Kerr effect (pMOKE). The photon energy of the linearly polarized laser beam ($h\nu = 1.51$ eV) was chosen slightly below the bandgap of the GaAs at 10 K; here, the specific Kerr rotation shows a maximum and the penetration depth of the light of more than 2 μm is significantly larger than the depletion depth of the GaAs (<200 nm). A square-wave bias voltage alternating between zero and V_b is applied between the two FeCo contacts and the Kerr rotation is detected synchronously with balanced photo-receivers and a lock-in technique. This ensures that the (quasistatic) magnetization of the FeCo contacts does not contribute to the Kerr signal.

The Kerr rotation angle, ϑ_K, versus the magnetic field applied along the [110] direction (z direction) at a distance of 1 μm from the edge of the left FeCo pad is shown in Fig. 1b (open triangles) for $V_b = -1{,}300$ mV. The Kerr signal very closely follows the magnetization of the FeCo injector, which clearly demonstrates that spins are indeed injected from the ferromagnetic contact into the semiconductor. The possibility of magnetic edge domains, which would seriously affect the spin-injection process can clearly be ruled out, as demonstrated by the behaviour seen in Fig. 1b, which is also observed at higher fields; that is, the magnetic moment does not increase beyond the value at 100 Oe (except a small increase due to the suppression of thermal spin waves).

DIRECT IMAGING OF THE SPIN DECAY

Figure 2a shows a colour-coded map of the saturation Kerr angle in the (110) plane obtained by an x–y scan across the cleaved edge. A decay of the spin polarization with increasing distance from the injector is observed, which is attributed to spin relaxation. This decay is exponential, and the decay length, L, varies as a function of the applied bias voltage from 5 to 30 μm (see Fig. 2b). This behaviour, which is in good agreement with the results in ref. 6, is assigned to the superposition of electron drift and spin diffusion[15]: when the electric field in the n channel is increased, the drift of the electrons supports (reverse bias) or attenuates (forward bias) the spread of spin polarization into the semiconductor. The decay length extrapolated to zero bias, that is, the spin diffusion length, is about 7 μm.

Measuring the spin polarization close to the left ('source') contact with positive bias, that is, with electrons flowing from the semiconductor into the FeCo contact, is equivalent to measuring the spin polarization at the drain contact for negative bias voltage because the distance between source and drain of 600 μm is much larger than the observed spin decay length. It is noteworthy that a sign reversal of the magneto-optical signal close to the source contact is observed when the bias voltage is changed from negative to positive, which was not seen in ref. 6. This raises the general question of the bias dependence of the injected spin polarization. From a physical point of view the more fundamental question is the effect of the electron kinetic energy on the spin-injection process. The electron energy, however, is not precisely known from the applied bias voltage for the sample geometry used here (and also in ref. 6) owing to the complex electric-field distribution in the sample resulting from the voltage drop across two Schottky barriers and the semiconductor channel.

Instead, we will discuss the bias dependence in a simpler device geometry, which is easily accessible in our 'cleave and observe' approach. The question of the sign reversal will be further discussed below.

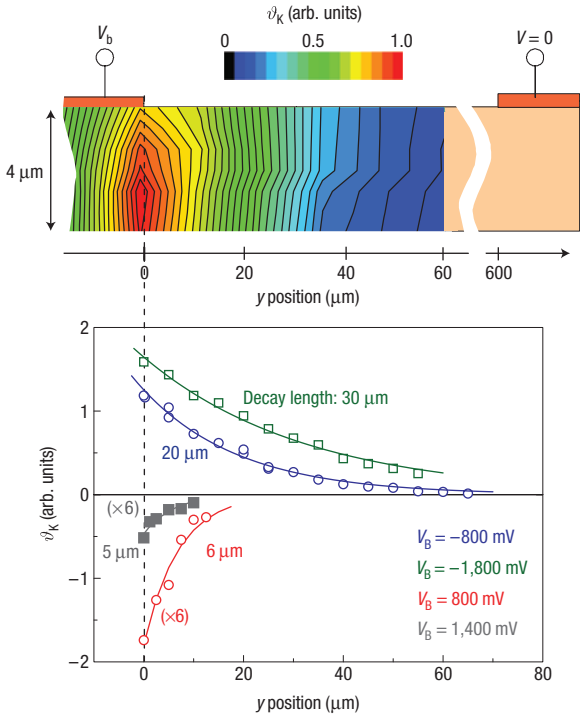

Figure 2 Cross-sectional imaging of the injected spin polarization in the lateral-current geometry (all measurements at $T = 9$ K). a, Colour-coded two-dimensional map of the Kerr signal amplitude for the geometry of Fig. 1a for $V_b = -1{,}300$ mV. **b**, One-dimensional Kerr scans along the *y* direction for different bias voltages. For forward bias ($V_b = 800$ mV and 1,400 mV) the Kerr rotation values have been multiplied by a factor of six for better visibility.

VERTICAL TRANSPORT OF ELECTRONS WITH WELL-DEFINED ENERGY

In the alternative sample design shown in Fig. 3a, the n^+ substrate itself constitutes the counter-electrode, and we thus avoid the effect of a non-uniform current density and the parasitic n-channel series resistance, which are intrinsic to the lateral geometry of Fig. 1a. The Kerr signal as a function of bias voltage is shown in Fig. 3b. Here, the bias voltage is equal to the voltage across the Schottky barrier; that is, eV_b now is the energy of the injected electrons. The Kerr rotation is proportional to $P_n = (n_{up} - n_{down})/(n_{up} + n_{down})$, which is the degree of electron spin polarization in the n-GaAs ($n_{up/down}$ being the density of spin-up/spin-down electrons). From this measurement we shall now extract the degree of spin polarization of the current J, that is, $P_j = (J_{up} - J_{down})/(J_{up} + J_{down})$.

In a first step we will relate the Kerr signal to the absolute value of electron spin polarization, P_n. Usually, P_n is determined by measuring the degree of circular polarization of the luminescence light resulting from the recombination of spin-polarized electrons and unpolarized holes. Because of a missing p-doped layer, which would provide itinerant holes, a combination of electroluminescence (EL) and photoluminescence (PL) is used, which was initially proposed in ref. 16: using a linearly polarized laser beam (wavelength $\lambda = 800$ nm) with the photon energy slightly above the bandgap of GaAs, unpolarized electron–hole pairs are generated in the n-GaAs. The holes recombine radiatively with available electrons, thus producing luminescence light with a degree of circular polarization half the degree of spin polarization of the recombining electrons. All measurements are made in the 'low-optical-pumping limit', that is, the dilution of spin-polarized electrons by optically excited unpolarized electrons can be ignored. This was verified by a variation of the intensity of the linearly polarized laser beam.

For this measurement the spin polarization is periodically reversed by switching the magnetization of the FeCo contact between the [110] and the $[\bar{1}\bar{1}0]$ direction while the polarization of the luminescent light is measured as a function of wavelength. Figure 3c shows the degree of circular polarization for $V_b = -50$ mV (red curve) and $V_b = +50$ mV (black curve). We obtain a non-zero circular polarization over the entire luminescence peak (814 nm $< \lambda <$ 822 nm; maximum intensity at 819 nm). The sign reversal of the light helicity when the bias voltage and hence the current direction is reversed shows that the spin polarization in the GaAs is indeed measured and any contribution from the metallic contacts can be ignored. This is further confirmed by the ratio of the signal values obtained for both polarities of V_b, which closely matches the respective Kerr rotation values shown in Fig. 3b.

The degree of circular polarization averaged over the luminescence peak for $V_b = -50$ mV is 0.075%, which translates into an average spin polarization $P_n = 0.15\%$ for the electrons contributing to the luminescence signal. As the spin polarization is known to be redistributed very efficiently between electrons[17], this should also be a good estimate for the spin polarization of the full electron system. The photoluminescence measurements also unambiguously show that the injected current for the materials used is carried by majority spin electrons.

Using this measurement, we are finally able to calibrate our Kerr data. The result is shown as a black curve in Fig. 3e. The low value of P_n is due to the fact that we inject relatively few polarized electrons into a semiconductor that already contains a large number of unpolarized electrons from the n doping.

To estimate P_j, that is, the efficiency of the electrical injection process itself, the local spin density resulting from the superposition of spin diffusion and electron drift has to be modelled. This is done on the basis of the drift–diffusion model in ref. 15. The extremely fast spin relaxation in the n^+ layer is taken into account by assuming the disappearance of the spin polarization of the electron density at the n/n^+ interface. The resistance of the n-GaAs layer is also assumed to be negligibly small compared with that of the Schottky barrier. Within this description, the electron spin polarization in the n channel is written as

$$P_n(x) = P_j \cdot \nu \cdot \frac{\exp\left(-\frac{x}{L_d}\right) - \exp\left(\frac{x}{L_u} - \frac{a}{L_d} - \frac{a}{L_u}\right)}{D \cdot \left(\frac{1}{L_d} + \frac{1}{L_u}\exp\left(-\frac{a}{L_d} - \frac{a}{L_u}\right)\right) + \nu\left(1 - \exp\left(-\frac{a}{L_d} - \frac{a}{L_u}\right)\right)}, \quad (1)$$

where $\nu = J/e \cdot n$ is the electron drift velocity, a is the thickness of the n channel, D is the diffusion constant and

$$L_{d/u} = \pm\frac{\nu \cdot \tau}{2} + \sqrt{\left(\frac{\nu\tau}{2}\right)^2 + D \cdot \tau}$$

is the upstream/downstream drift–diffusion length, τ being the spin relaxation time. To test the validity of this formula, we carried out one-dimensional Kerr effect scans in the $[00\bar{1}]$ direction for three different bias voltages (data points in Fig. 3d) and measured the depolarization under a small magnetic field applied along the x direction (the so-called Hanle curve; data points in the inset of Fig. 3d; see the Supplementary Information). The curves show an enhanced spin relaxation compared with the geometry of Fig. 1a,

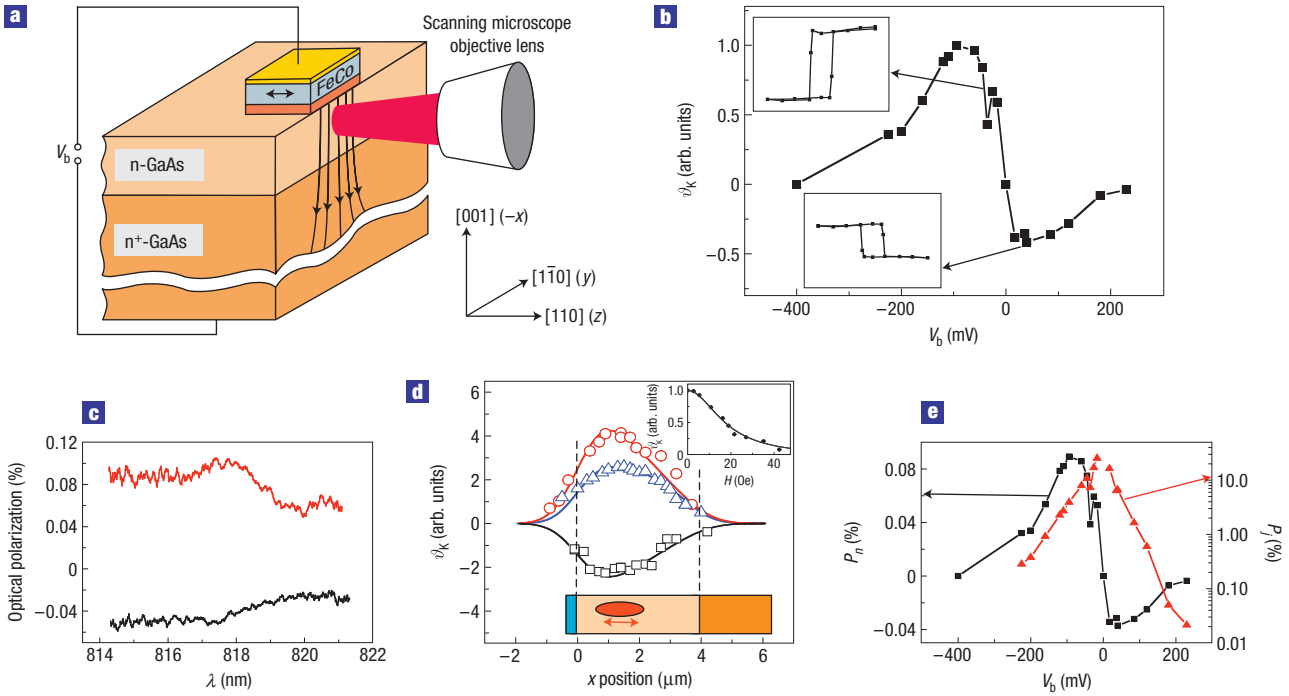

Figure 3 Characterization of the injected spin polarization in the vertical-current geometry. a, Sample design for vertical-current measurements where—in contrast to the lateral geometries in Fig. 1 or in refs 6,22—the energy of the injected electrons, ε_e, to a very good approximation is given by the bias voltage ($\varepsilon_e = eV_b$). **b**, Kerr rotation amplitude versus applied bias voltage for the sample of **a** measured in the n channel. The insets clearly show the change of sign in the Kerr rotation versus magnetic field. **c**, Degree of circular polarization of the light emitted by a combination of electroluminescence (EL) and photoluminescence (PL) of the n channel for $V_b = -50$ mV (red) and for $V_b = +50$ mV (black) for optical excitation at a wavelength of 800 nm for the sample of **a**. **d**, One-dimensional Kerr scans in the vertical direction ($x \parallel [001]$) for the sample of **a** for bias voltages of −40 mV (red circles), −200 mV (blue triangles) and +50 mV (black squares). The solid lines represent the calculated Kerr signals taking into account the gaussian profile of the laser spot and a spin-density profile on the basis of equation (1) for the respective bias voltages. The inset shows the spin polarization as a function of a small transverse magnetic field applied in the x direction (data points) and a numerical fit (solid line) taking into account the precession around the magnetic field (Hanle effect; see the Supplementary Information). Resulting fit parameters are $D = 5\,\mathrm{cm^2\,s^{-1}}$ and $\tau = 100$ ns. **e**, The spin polarization of the electron density (P_n, black) is deduced from **b** using the luminescence data of **c** as a calibration; the spin polarization of the current (P_j, red) is deduced from P_n by using equation (1). Here—in contrast to the data in Fig. 2b—the bias voltage, V_b, directly defines the energy of the injected electrons eV_b. All measurements are made at a distance of 1 μm below the FeCo contact (except in **d**) at a temperature $T = 9$ K.

that is, a shorter spin decay length and broader Hanle curve, which is attributed to the diffusion of electron spins into the n^+ substrate. The observed decay was indeed reproduced using equation (1) with $D = 5\,\mathrm{cm^2\,s^{-1}}$ and $\tau = 100$ ns, in good agreement with published values for n-GaAs (refs 6,18,19). The Hanle curve was reproduced using the same parameters and inserting the term describing the precession around the transverse field in equation (1).

THE ROLE OF BIAS VOLTAGE

The spin polarization of the current, P_j, deduced from P_n using equation (1) is shown in Fig. 3e in red. A sharp peak centred close to zero bias with a maximum value about 30% and a full width at half maximum of the order of 50 mV is observed. As the influence of electron drift was removed by the analysis presented above, we believe that this pronounced bias dependence originates from the electrical spin-injection process itself.

Spin injection arises from the asymmetry between the spin-up (majority) and spin-down (minority) electronic states near the Fermi level, E_F, of the ferromagnet: owing to this asymmetry, for reverse bias ($V_b < 0$) electrons with one spin polarization will dominate the tunnelling current from the ferromagnet into the semiconductor; for forward bias ($V_b > 0$) the current tunnelling into the ferromagnet from an unpolarized semiconductor is also spin polarized, resulting in a spin accumulation in the semiconductor due to electrons not transmitted through the barrier[20,21]. Therefore, the spin polarization observed in the semiconductor, P_n, when the bias voltage and the current direction are reversed, is related to electrons in the majority and minority spin bands of the ferromagnet at $E_F + eV_b$ (forward bias) and at $\approx E_F$ (reverse bias). For the likely case that the spin polarization in the ferromagnet does not change sign between E_F and $E_F + eV_b$, an opposite sign of P_n in the semiconductor is expected for forward and reverse bias, respectively. This is indeed observed in the present experiment for an $Fe_{32}Co_{68}(001)$ injector. Crooker *et al.*[6], however, who used an Fe(001) injector, did not see a sign reversal of $P_n(V_b)$. This is an unexpected behaviour, because the spin polarization close to E_F should not be fundamentally different for Fe and b.c.c.-FeCo. In fact, in a more recent experiment with a non-local geometry of Fe contacts on GaAs, the same authors observed a sign reversal of the spin polarization in the semiconductor when changing from reverse to forward bias[22], but only for small bias voltages (<100 mV) and with positive or negative zero-crossing points for different samples. It is not clear at this moment whether the observed bias dependence of the spin polarization is determined by different

growth conditions of the ferromagnet (see the Methods section) and possible surface bands at the Schottky barrier[23], or by the higher band filling for FeCo compared with Fe. *Ab initio* band calculations of electronic states and electron transport at the Fe/GaAs and FeCo/GaAs interfaces, therefore, seem indispensable to quantitatively understand the details of spin injection from a 3d ferromagnet into a semiconductor.

TOWARDS A FUNCTIONAL SPIN-FET

To implement a working spin-FET as proposed in ref. 2 a number of criteria will have to be fulfilled with respect to materials properties, device design and operating conditions[1]. For certain important steps towards a functional spin-FET the experimental methods presented above are expected to be helpful. (1) Two stable states with parallel and antiparallel remanent magnetization of the source and drain contacts are easily realized using our previous experience in tuning the magnetic anisotropy and coercivity of epitaxial ferromagnetic layers[14]. (2) A voltage applied to a gate electrode above the channel will modulate the source–drain current via spin precession due to the Bychkov–Rashba effect[1]. In contrast to earlier imaging methods[6,22], the present approach enables us to observe the two-dimensional spin distribution below the gate and will thus help to interpret the magneto-resistive effects. (3) A two-dimensional electron gas (2DEG) as the conducting channel will ensure a uniform Rashba precession. The scheme for spin injection used in the present experiment should equally work for a 2DEG; the sensitivity of our Kerr measurement is sufficient to detect spin injection in a 2DEG with a typical electron density of several times 10^{11} cm^{-2}. (4) The channel length must be well below the downstream spin decay length, L_d (for example $\leq 10\,\mu$m, see Fig. 2) and short enough to avoid a cancellation of the resulting spin polarization at the end of the channel due to the distribution of electron wavevectors in the y–z plane. According to refs 24,25 the spin precession should be observable with our resolution and sensitivity for a channel length up to a few micrometres even for diffusive transport at $T \leq 77$ K.

Furthermore, appropriate values for a number of parameters (electron mobility, Bychkov–Rashba parameter, channel versus contact resistance, gate breakdown voltage and so on) must be achieved to allow for a Rashba precession period smaller than the channel length and for a sufficiently large modulation of the source–drain current. It is expected that the novel imaging method introduced in the present work will be a useful tool to solve complex materials and design problems and thus help to develop and optimize a functional spin-FET or other future spintronic devices[1].

METHODS

For the sample design according to Fig. 1a, a semi-insulating GaAs(001) wafer was used as substrate. A 4-μm-thick GaAs layer n-doped with Si ($n = 10^{16}$ cm^{-3}) was grown by molecular beam epitaxy (MBE) under standard conditions followed by a 15-nm-thick transition layer, where the doping level was continuously increased from $n = 10^{16}$ cm^{-3} to $n = 4 \times 10^{18}$ cm^{-3}, and by a 15-nm-thick n$^+$-layer with $n = 4 \times 10^{18}$ cm^{-3} to obtain a narrow Schottky barrier. After capping with an amorphous As layer, the samples were transferred into a second MBE chamber. The As was then desorbed by heating to about 500 °C until the reflection high-energy electron diffraction pattern of the characteristic (4×6) reconstruction of the GaAs(001) surface was seen with sharp spots forming Laue circles, thus indicating a clean and extremely flat surface[14,26]. Then a 14-nm-thick $Fe_{32}Co_{68}$(001) film was grown by MBE at room temperature and covered with 10 nm Au for protection. Epitaxial growth and orientation of the metallic films were verified by reflection high-energy electron diffraction.

Optical lithography and Ar ion etching were used to form two contacts of the metallic films (size 200 μm × 400 μm) with a 600 μm gap in between. Secondary-ion mass spectroscopy was used during the etching process to verify the complete removal of the metallic layers. The n$^+$-GaAs layer and the n to n$^+$ transition layer were removed everywhere except under the metallic contacts. Finally, a wet-chemical-etching process with citric acid was applied to remove material with high defect density. The wafer was then cleaved along the [1$\bar{1}$0] direction across the FeCo pads, leaving two contacts with dimensions of 100 μm × 400 μm, which were then wire bonded for subsequent electrical measurements.

For the sample shown in Fig. 3a, an n$^+$-doped GaAs substrate ($n = 10^{18}$ cm^{-3}) was used without a buffer layer; otherwise, the same procedure was applied for film deposition and patterning of a single metallic contact pad.

For the magneto-optic measurements, the beam of a Ti-sapphire laser was focused on the cleaved edge of the samples by means of a scanning optical microscope after passing through a linear polarizer. A spatial resolution of 1.6 μm was obtained. The photon energy was tuned to $h\nu = 1.51$ eV, which is close to the maximum of the saturation Kerr rotation angle, ϑ_K, for our sample at $T = 9$ K. The Kerr rotation of the beam reflected from the cleaved edge after passing through the microscope objective lens and a beam splitter was measured with a Wollaston prism and a pair of balanced photo-receivers. A square-wave bias voltage alternating between zero and V_b with a frequency of 6 kHz was applied between the two FeCo contacts; the Kerr rotation angle was detected synchronously using a lock-in technique.

For the measurement of the circular polarization shown in Fig. 3c, the magnetization of the FeCo contact was periodically reversed between the two easy directions, [110] and [1$\bar{1}$0], by short magnetic-field pulses (pulse width 200 μs, pulse height ±150 Oe) with a frequency of 10 Hz. Using a combination of a quarter-wave plate, a linear polarizer and a CCD (charge-coupled device) spectrometer, the circular polarization of the luminescent light for a given bias voltage was measured by synchronous detection as a function of wavelength. Data acquisition was always done at remanence.

Received 2 January 2007; accepted 6 September 2007; published 7 October 2007.

References

1. Žutić, I., Fabian, J. & Das Sarma, S. Spintronics: Fundamental and applications. *Rev. Mod. Phys.* **76**, 323–410 (2004).
2. Datta, S. & Das, B. Electronic analog of the electro-optic modulator. *Appl. Phys. Lett.* **56**, 665–667 (1990).
3. Zhu, H. J. *et al.* Room-temperature spin injection from Fe into GaAs. *Phys. Rev. Lett.* **87**, 016601 (2001).
4. Hanbicki, A. T., Jonker, B. T., Itskos, G., Kioseoglou, G. & Petrou, A. Efficient electrical spin injection from a magnetic metal/tunnel barrier contact into a semiconductor. *Appl. Phys. Lett.* **80**, 1240–1242 (2002).
5. Adelmann, C., Lou, X., Strand, J., Palmstrøm, C. J. & Crowell, P. A. Spin injection and relaxation in ferromagnet–semiconductor heterostructures. *Phys. Rev. B* **71**, 121301 (2005).
6. Crooker, S. A. *et al.* Imaging spin transport in lateral ferromagnet/semiconductor structures. *Science* **309**, 2191–2195 (2005).
7. Motsnyi, F. *et al.* Electrical spin injection in a ferromagnet/tunnel barrier/semiconductor heterostructure. *Appl. Phys. Lett.* **81**, 265–267 (2002).
8. Jiang, X. *et al.* Highly spin-polarized room-temperature tunnel injector for semiconductor spintronics using MgO (100). *Phys. Rev. Lett.* **94**, 056601 (2005).
9. Adelmann, C. *et al.* Spin injection from a perpendicular magnetized ferromagnetic δ-MnGa into (Al,Ga)As heterostructures. *Appl. Phys. Lett.* **89**, 112511 (2006).
10. Gerhardt, N. C. *et al.* Electron spin injection into GaAs from ferromagnetic contacts in remanence. *Appl. Phys. Lett.* **87**, 032502 (2005).
11. van 't Erve, O. M. J., Kioseoglou, G., Hanbicki, A. T., Li, C. H. & Jonker, B. T. Remanent electrical spin injection from Fe into AlGaAs/GaAs light emitting diodes. *Appl. Phys. Lett.* **89**, 072505 (2006).
12. Lou, X. *et al.* Electrical detection of spin accumulation at a ferromagnet–semiconductor interface. *Phys. Rev. Lett.* **96**, 176603 (2006).
13. Padovani, F. A. & Stratton, R. Field and thermionic-field emission in Schottky barriers. *Solid-State Electron.* **9**, 695 (1966).
14. Bayreuther, G., Dumm, M., Uhl, B., Meier, R. & Kipferl, W. Magnetocrystalline volume and interface anisotropies in epitaxial films: Universal relation and Néel's model. *J. Appl. Phys.* **93**, 8230–8235 (2003).
15. Yu, Z. G. & Flatté, M. E. Spin diffusion and injection in semiconductor structures: Electric field effects. *Phys. Rev. B* **66**, 235302 (2002).
16. Aronov, A. G. & Pikus, G. E. Spin injection into semiconductors. *Sov. Phys. Semicond.* **10**, 698–700 (1976).
17. Paget, D. & Berkovits, V. L. in *Optical Orientation* (eds Meier, F. & Zakharchenya, B. P.) Ch. 9, 381–422 (North-Holland, Amsterdam, 1984).
18. Kikkawa, J. M. & Awschalom, D. D. Resonant spin amplification in n-type GaAs. *Phys. Rev. Lett.* **80**, 4313–4316 (1998).
19. Dzhioev, R. I. *et al.* Low-temperature spin relaxation in n-type GaAs. *Phys. Rev. B* **66**, 245204 (2002).
20. Ciuti, C., McGuire, J. P. & Sham, L. J. Spin polarization of semiconductor carriers by reflection off a ferromagnet. *Phys. Rev. Lett.* **89**, 156601 (2002).
21. Osipov, V. V. & Bratkovsky, A. M. Spin accumulation in degenerate semiconductors near modified Schottky contact with ferromagnets: Spin injection and extraction. *Phys. Rev. B* **72**, 115322 (2005).
22. Lou, X. *et al.* Electrical detection of spin transport in lateral ferromagnet–semiconductor devices. *Nature Phys.* **3**, 197–202 (2007).
23. Dery, H. & Sham, L. J. Spin extraction theory and its relevance to spintronics. *Phys. Rev. Lett.* **98**, 046602 (2007).

24. Bournel, A., Dollfus, P., Bruno, P. & Hesto, P. Spin polarized transport in 1D and 2D semiconductor heterostructures. *Mater. Sci. Forum* **297–298**, 205–212 (1999).
25. Bournel, A., Dollfus, P., Bruno, P. & Hesto, P. Gate-induced spin precession in an $In_{0.53}Ga_{0.47}As$ two dimensional electron gas. *Eur. Phys. J. AP* **4**, 1–4 (1998).
26. Moosbühler, R., Bensch, F., Dumm, M. & Bayreuther, G. Epitaxial Fe films on GaAs(001): Does the substrate surface reconstruction affect the uniaxial magnetic anisotropy? *J. Appl. Phys.* **91**, 8757–8759 (2002).

Acknowledgements

This work has been supported by the Deutsche Forschungsgemeinschaft (DFG) under FOR 370 and SFB 689. We thank B. Muermann and J. Ehehalt for assistance with programming some of the measurement procedures, P. Chen for characterization of the GaAs materials and J. Fabian for discussions.

Correspondence and requests for materials should be addressed to G.B.
Supplementary Information accompanies this paper on www.nature.com/naturephysics.

Author contributions

P.K. designed and carried out the experiments, analysed the data and prepared the manuscript; M.B. conceived the main experiment, developed the theoretical data analysis and contributed to the manuscript; M.S. carried out the SQUID measurements and contributed to the manuscript; A.S. carried out part of the sample preparation; D.S. grew the semiconductor materials; W.W. devised the project and contributed materials; C.H.B. provided support for the optical measurements and contributed to the manuscript; G.B. devised the project, contributed to the data analysis and wrote the paper.